Advances in Aircraft and Spacecraft Science, *Vol. 7, No. 4 (2020) 291-308*
DOI: https://doi.org/10.12989/aas.2020.7.4.291

Effect of dynamic absorber on the nonlinear vibration of SFG cylindrical shell

Kamran Foroutan[a] and Habib Ahmadi*

Faculty of Mechanical Engineering, Shahrood University of Technology, Shahrood, Iran

(Received October 27, 2019, Revised January 9, 2020, Accepted January 14, 2020)

Abstract. In this paper, a numerical method is utilized to study the effect of a new vibration absorber on vibration response of the stiffened functionally graded (SFG) cylindrical shell under a couple of axial and transverse compressions. The material composition of the stiffeners and shell is continuously changed through the thickness. The vibration absorber consists of a mass-spring-damper system which is connected to the ground utilizing a linear local damper. To simplify, the spring element of the vibration absorber is called global potential. The von Kármán strain-displacement kinematic nonlinearity is employed in the constitutive laws of the shell and stiffeners. To consider the stiffeners in the model, the smeared stiffener technique is used. After obtaining the governing equations, the Galerkin method is applied to discretize the nonlinear dynamic equation of system. In order to find the nonlinear vibration responses, the fourth order Runge-Kutta method is utilized. The influence of the stiffeners, the dynamic absorber parameters on the vibration behavior of the SFG cylindrical shell is investigated. Also, the influences of material parameters of the system on the vibration response are examined.

Keywords: SFG cylindrical shell; dynamic absorber; nonlinear vibration response; compression loading

1. Introduction

The FG materials are utilized wildly in a various applications of engineering. These structures are utilized in the aerospace, fusion energy devices, engine combustion chambers, engine parts, and other engineering structures. In this regard, the stiffened FG cylindrical shells are utilized impressively in various engineering industries including bridges, submarines, satellites, aircraft, offshore, and ships structures. Another device that is wildly used in various branches of industries to vibration suppression is the vibration absorber. Absorbers are applicable devices for passively reducing the amplitude of vibrations. These absorbers have various types and strongly are used in the engineering applications with high efficiency. Also, these devices are used in various industries such as the aerospace industry, bridges, building project, etc.

For the dynamic behavior of the plates and shells, the vibration behaviors of cylindrical shells with FG material under axial excitation were presented by Ng *et al.* (2001). Wang *et al.* (2016) addressed the linear and nonlinear free vibrations of an axially moving rectangular plate coupled with dense fluid having a free surface. The vibrations of FG rectangular plates with porosities and

---

*Corresponding author, Ph.D., E-mail: habibahmadif@shahroodut.ac.ir
[a]Ph.D. Student, E-mail: kamran.foroutan@shahroodut.ac.ir

http://www.techno-press.org/?journal=aas&subpage=7 ISSN: 2287-528X (Print), 2287-5271 (Online)

moving in thermal environment were studied by Wang and Zu (2017a). Also, Wang and Zu (2017b) presented the nonlinear steady-state responses of longitudinally traveling FG plates immersed in liquid. Meng *et al.* (2016) investigated the non-axisymmetric dynamic buckling of cylindrical shells under the axial step load. They used the FSD theory, the Ritz, and Variable Separation methods. Wang *et al.* (2018) presented the free thermal vibration of FG cylindrical shells containing porosities. Sofiyev (2009, 2004) addressed the vibration behavior of FG truncated conical and cylindrical shells under the periodic and non-periodic impulsive loads, respectively. Wang (2018) studied the electro-mechanical vibration analysis of functionally graded piezoelectric porous plates in the translation state. Wang *et al.* (2019a) investigated the nonlinear dynamics of fluid-conveying FG sandwich nanoshells. The vibration response of cylindrical shell with FG material under a linear axial loading in thermal environments was presented by Huang and Han (2010). Wang *et al.* (2019b) analyzed the nonlinear vibration behavior of metal foam circular cylindrical shells reinforced with graphene platelets. Also, Wang *et al.* (2013) studied the nonlinear vibrations of a thin, elastic, laminated composite circular cylindrical shell, moving in axial direction and having an internal resonance. The nonlinear vibrations of rotating, laminated composite circular cylindrical shells subjected to radial harmonic excitation in the neighborhood of the lowest resonances are investigated by Wang (2014). The nonlinear vibrations of longitudinally moving FG plates containing porosities and contacting with liquid were studied by Wang and Yang (2017).

Previous studies mentioned above illustrate that the influence of stiffeners on the vibration of cylindrical shells with FG material has not been addressed. But, some researchers have been studied the influence of stiffeners on dynamic behavior of SFG cylindrical shells.

The dynamic and static behaviors of SFG plates, cylindrical, and shallow shells were investigated by Bich *et al.* (2011, 2013). The vibration behaviors of SFG cylindrical shells resting on an elastic medium under external excitation were presented by Van Dung and Nam (2014). Duc and Thang (2015) studied an analytical method to analyze the vibration behavior of imperfect SFG cylindrical shells resting on the elastic medium subjected to the damping and mechanical loads.

Few studies have been performed about the influences of absorbers on the vibration response of cylindrical shells. For instance, Huang and Fuller (1997) considered the influence of absorbers on the vibration response of the cylindrical shell. They used multiple dynamic absorbers to suppress the vibration response of the system. Design and implementation of a time-varying shunted electromagnetic tunable vibration absorber for broadband vibration control of cylindrical shell were investigated by Turco and Gardonio (2017). Huang and Chen (2000) studied the influence of absorbers on the suppression of vibration response of the thin elastic cylindrical shell. Pandy and Koss (1984) investigated the effectiveness of roller supports acting simultaneously as vibration absorbers on the reduction of broadband noise radiated from cylindrical shells.

A literature review illustrates that few researches have been addressed the investigation of vibration response of stiffened functionally graded cylindrical shell equipped with a vibration absorber. In this work, the influence of new vibration absorber consists of linear spring that globally is connected to the FG cylindrical shell and a linear local damper that is connected to the ground. The effect of this absorber on the vibration response of the SFG cylindrical shell under a couple of axial and transverse compression is presented using the numerical approach. The material composition of shell and stiffeners is continuously changed through the thickness. The relations of strain-displacement are derived according to the von Kármán equations and classical shell theory. After obtaining the governing equations, the Galerkin method is utilized to discretize the nonlinear dynamic equation of system. In order to find the nonlinear vibration responses, the fourth order Runge-Kutta method is utilized. Results are represented to examine the influence of stiffeners, vibration absorber and material properties on the vibration behavior of cylindrical shells with FG material.

2. Theoretical formulation

2.1 FG material properties

Configuration of the SFG cylindrical shell with a dynamic absorber is illustrated in Fig. 1. Coordinates $y = R\theta$ and x represent the circumferential and the axial direction of the cylindrical shell and z is the radial direction (Fig. 1). According to Fig. 1, the coordinate system ($x, y,$ and z) is attached to the left end of the middle surface of the system. The geometrical of shell h, L and R are the thickness, axial length, and radius, respectively. For stiffeners s_i, d_i and h_i ($i = r, s$) are the spacing, width, and thickness, respectively. The subscripts r and s refer to ring and stringer stiffeners, respectively. The absorber with spring stiffness k, mass m, and damping coefficient c is located in $x = d$. The FG internal stiffeners and cylindrical shell are composed of metals and ceramics. It is considered that the inner shell surface is ceramic and the outer surface is metal, and for stiffeners, it is selected as reverse order.

The volume fractions of the constituents regarding the power law are defined as (Ebrahimi and Heidari 2018, Shaterzadeh *et al.* 2019, Sayyad and Ghugal 2018, Shegokara and Lal 2016)

$$\begin{aligned} V_c &= V_c(z) = \left(\frac{2z+h}{2h}\right)^N \\ V_m &= V_m(z) = 1 - V_c(z) \end{aligned} \tag{1}$$

where V_c and V_m refer to the ceramic and metal volume fractions. $N \geq 0$ is the material power law index of the FG shell. $\mathrm{P_{eff}}$ (effective properties) is expressed as (Foroutan *et al.* 2018)

$$\mathrm{P}_{eff} = \mathrm{P}_m(z)V_m(z) + \mathrm{P}_c(z)V_c \tag{2}$$

Due to the mentioned law, the mass density and Young's modulus of the shell and stiffeners are defined as follows (Hong 2014, Zenkour and Aljadani 2018)

$$\begin{aligned} E(z) &= E_m + (E_c - E_m)\left(\frac{2z+h}{2h}\right)^N, -\frac{h}{2} \leq z \leq \frac{h}{2} \\ \rho(z) &= \rho_m + (\rho_c - \rho_m)\left(\frac{2z+h}{2h}\right)^N, -\frac{h}{2} \leq z \leq \frac{h}{2} \end{aligned} \tag{3a}$$

$$\left.\begin{aligned} E_i(z) &= E_c + (E_m - E_c)\left(\frac{2z-h}{2h_i}\right)^{N_i}, \frac{h}{2} \leq z \leq \left(\frac{h}{2} + h_i\right) \\ \rho_i(z) &= \rho_c + (\rho_m - \rho_c)\left(\frac{2z-h}{2h_i}\right)^{N_i}, \frac{h}{2} \leq z \leq \left(\frac{h}{2} + h_i\right) \end{aligned}\right. ; i = s, r \tag{3b}$$

where E_i, E are Young's modulus and ρ_i, ρ are the mass density of functionally graded stiffeners and shell, respectively. Also, N_i is the material power law index of the FG stiffeners.

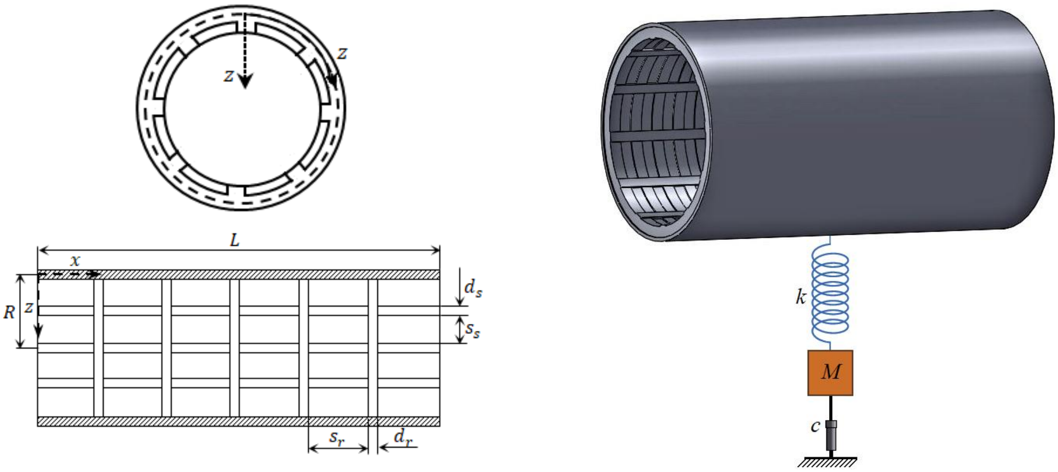

Fig. 1 Configuration of SFG cylindrical shell

2.2 Governing equations

The equilibrium equations of cylindrical shells based on the classical shell theory are as follows (Van Dung and Nam 2014, Foroutan *et al.* 2019, 2020, Gonçalves and Del Prado 2005, Volmir 1972)

$$\begin{aligned} &N_{x,x}+N_{xy,y}=0 \\ &N_{xy,x}+N_{y,y}=0 \\ &M_{x,xx}+2M_{xy,xy}+M_{y,yy}+N_xw_{,xx}+2N_{xy}w_{,xy}+N_yw_{,yy}+\frac{1}{R}N_y=\rho_1 w_{,tt} \end{aligned} \tag{4}$$

In the present study, the vibration absorber is utilized to the vibration suppression of SFG cylindrical shell. Therefore, with regard to Eq. (4), the governing equation considering stiffened shell and absorber dynamic is derived as follows

$$\begin{aligned} &N_{x,x}+N_{xy,y}=0 \\ &N_{xy,x}+N_{y,y}=0 \\ &M_{x,xx}+2M_{xy,xy}+M_{y,yy}+N_xw_{,xx}+2N_{xy}w_{,xy}+N_yw_{,yy}+\frac{1}{R}N_y \\ &\quad+\left[2\rho_1 cw_{,t}-k\left(s-w\right)\right]\delta_k\left(x-d,y-R\pi/2\right)=\rho_1 w_{,tt} \\ &Ms_{,tt}+\left[k\left(s-w\right)+cs_{,t}\right]\delta_k\left(x-d,y-R\pi/2\right)=0 \end{aligned} \tag{5}$$

where subscript t refers to the time, δ_k is Dirac delta and ρ_1 is the mass density which can be obtained as

$$\rho_1=\left(\rho_m+\frac{\rho_c-\rho_m}{N+1}\right)h+\left(\rho_c+\frac{\rho_m-\rho_c}{N_s+1}\right)\frac{A_s}{S_s}+\left(\rho_c+\frac{\rho_m-\rho_c}{N_r+1}\right)\frac{A_r}{S_r} \tag{6}$$

According to the first and second relations of Eq. (5), the resultant forces in terms of stress function (φ) are defined as follows

$$N_x = \varphi_{,yy}, \; N_y = \varphi_{,xx}, \; N_{xy} = -\varphi_{,xy} \tag{7}$$

Regarding the references (Van Dung and Nam 2014, Foroutan *et al.* 2019) and substituting Eq. (7) in the last two of Eq. (5), the governing equations of system can be obtained as

$$\begin{aligned} &A_{11}^*\varphi_{,xxxx} + \left(A_{33}^* - 2A_{12}^*\right)\varphi_{,xxyy} + A_{22}^*\varphi_{,yyyy} + A_{24}^*w_{,xxxx} + \left(A_{14}^* + A_{25}^* - 2A_{36}^*\right)w_{,xxyy} \\ &+ A_{15}^*w_{,yyyy} + \frac{1}{R}w_{,xx} - \left[\left(w_{,xy}\right)^2 - w_{,xx}w_{,yy}\right] = 0 \end{aligned} \tag{8}$$

$$\begin{aligned} &\rho_1 w_{,tt} + 2\rho_1 c w_{,t}\delta_k\left(x-d, y-R\pi/2\right) + A_{44}^*w_{,xxxx} + \left(A_{45}^* + A_{54}^* + 4A_{66}^*\right)w_{,xxyy} \\ &+ A_{55}^*w_{,yyyy} - A_{24}^*\varphi_{,xxxx} - \left(A_{14}^* + A_{25}^* - 2A_{36}^*\right)\varphi_{,xxyy} - A_{15}^*\varphi_{,yyyy} - \frac{1}{R}\varphi_{,xx} \\ &- \varphi_{,yy}w_{,xx} + 2\varphi_{,xy}w_{,xy} - \varphi_{,xx}w_{,yy} - k\left(s-w\right)\delta_k\left(x-d, y-R\pi/2\right) = 0 \end{aligned} \tag{9}$$

$$Ms_{,tt} + \left[k\left(s-w\right) + cs_{,t}\right]\delta_k\left(x-d, y-R\pi/2\right) = 0 \tag{10}$$

where the coefficients A_{ij}^* are defined in Appendix.

2.2.1 Boundary conditions

Suppose that a SFG cylindrical shell is simply supported and subjected to a couple of transverse and axial periodic compressions. Thus the boundary conditions are of the form

$$w = 0, M_x = 0, \; N_x = -P_x h, \; N_y = -P_y h, \; N_{xy} = 0 \; at \; x = 0; L \tag{11}$$

The shells deflection regarding the boundary condition is considered as follows (Bich *et al.* 2012, Volmir 1972, Sofiyev and Schnack 2004)

$$w = \sum_m \sum_n W\left(t\right)\sin\alpha_m x \, \sin\beta_n y \tag{12}$$

where $\alpha_m = \dfrac{m\pi}{L}$; $\beta_n = \dfrac{n}{R}$ and $W(t)$ is time-dependent amplitude, n is the number of full wave in the circumferential direction and m is the half wave in the axial direction.

Eq. (12) is substituted in Eq. (8) and the resulting equation is solved to find the unknown stress function (φ) as follows

$$\varphi = \varphi_1\cos 2\alpha_m x + \varphi_2\cos 2\beta_n y - \varphi_3\sin\alpha_m x\,\sin\beta_n y - P_X h\frac{y^2}{2} - P_y h\frac{x^2}{2} \tag{13}$$

where P_y and P_x are the average circumferential and axial stresses, respectively. The coefficients $\varphi_i (i = 1,2,3)$ are in the following form

$$\varphi_1 = \frac{n^2\lambda^2}{32A_{11}^*m^2\pi^2}W^2; \quad \varphi_2 = \frac{m^2\pi^2}{32A_{22}^*n^2\lambda^2}W^2; \quad \varphi_3 = \frac{B}{A}W \tag{14}$$

where coefficients A, B are defined in Appendix.

If Eqs. (9) and (10) are denoted by G_1 and G_2, respectively, the ordinary differential equation of system may be found in terms of W and s using Galerkin's method in the following form

$$\begin{aligned}&\int_0^L \int_0^{2\pi R} \sin\alpha_m x \sin\beta_n y\, \Gamma_1 dydx = 0\\&\int_0^L \int_0^{2\pi R} \sin\alpha_m x \sin\beta_n y\, \Gamma_2 dydx = 0\end{aligned} \tag{15}$$

After substitution of Eqs. (12) and (13) into Eq. (15), the following results may be obtained, after carrying out mentioned integrations and some simplification, Eq. (15) can be written as follows

$$\ddot{W} + a_1 W + a_2 W^3 + a_3 kW + a_4 ks - \left(a_5 P_X + a_6 P_y\right) W = 0 \tag{16}$$

$$\ddot{s} + b_1 ks + b_2 c\dot{s} + b_2 kW = 0 \tag{17}$$

where

$$\begin{aligned}&a_1 = \frac{\left(D + \dfrac{BB^*}{A}\right)}{\rho_1 L^4};\ a_2 = \frac{G}{\rho_1 L^4};\ a_3 = \frac{2}{R\pi L\rho_1}\left(\sin\left(\frac{n\pi}{2}\right)\sin\left(\frac{m\pi d}{L}\right)\right)^2\\&a_4 = \frac{-2}{R\pi L\rho_1}\sin\left(\frac{n\pi}{2}\right)\sin\left(\frac{m\pi d}{L}\right);\ a_5 = \frac{m^2\pi^2 h}{\rho_1 L^2};\ a_6 = \frac{n^2 h}{R^2\rho_1}\\&b_1 = \frac{-1}{M}\left(\sin\left(\frac{n\pi}{2}\right)\sin\left(\frac{m\pi d}{L}\right)\right)^2;\ b_2 = \frac{1}{M}\sin\left(\frac{n\pi}{2}\right)\sin\left(\frac{m\pi d}{L}\right)\end{aligned} \tag{18}$$

where coefficients G, B^* and D are presented in Appendix.

2.3 Free vibration analysis

For the linear and free vibration analysis of the FG stiffened shell, vibration absorbers, and periodic load in Eq. (16) are ignored, therefore, Eq. (15) reduces to

$$\ddot{W} + a_1 W = 0 \tag{19}$$

According to Eq. (19), natural frequencies of system are obtained as

$$\omega_n = \sqrt{a_1} \tag{20}$$

The natural frequency in Eq. (19) is used to validate the present formulations. Also, in order to find the critical natural frequency of the SFG cylindrical shell, the minimum value of natural frequencies should be obtained. The critical mode number can be obtained regarding this value for the SFG cylindrical shell. It should be noted that for calculating the nonlinear vibration response, the middle deflection of the shell is considered which is shown by $W_{\max}$ in the presented figures.

3. Numerical results

3.1 Validation of this study

Table 1 Comparison of the natural frequencies of cylindrical shell

m	n	Present	Qin *et al.* (2017)		Pellicano (2007)		Wang *et al.* (2019c)	
				Errors (%)		Errors (%)		Errors (%)
1	7	486.0	484.6	0.2	484.6	0.2	484.55	0.2
1	8	490.3	489.6	0.1	489.6	0.1	489.55	0.1
1	9	545.8	546.2	0.07	546.2	0.07	546.20	0.07
1	6	555.8	553.3	0.4	553.3	0.4	553.33	0.4
1	10	634.8	636.8	0.3	636.8	0.3	636.81	0.3
1	5	728.5	722.1	0.8	722.1	0.8	722.13	0.8
1	11	746.6	750.7	0.5	750.7	0.5	750.66	0.5
1	12	875.5	882.2	0.7	882.2	0.7	882.23	0.7
2	10	962.3	968.1	0.5	968.1	0.5	968.09	0.5
2	11	976.6	983.4	0.6	983.4	0.6	983.34	0.6

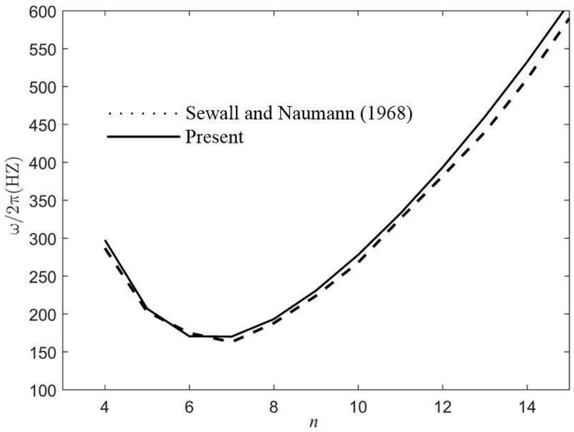

Fig. 2 Comparison of the natural frequencies of isotropic un-stiffened cylindrical shell ($m = 1$)

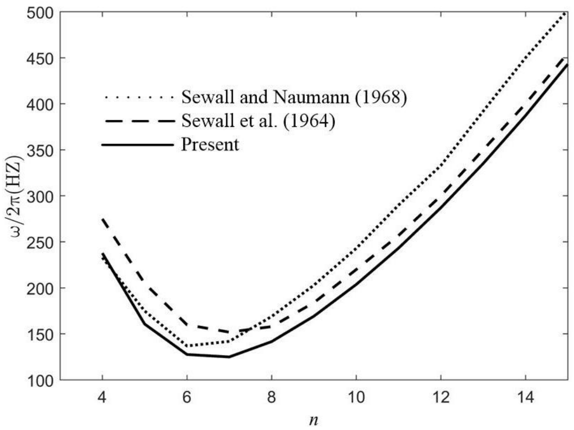

Fig. 3 Comparison of the natural frequencies of isotropic internal stiffened cylindrical shell ($m = 1$)

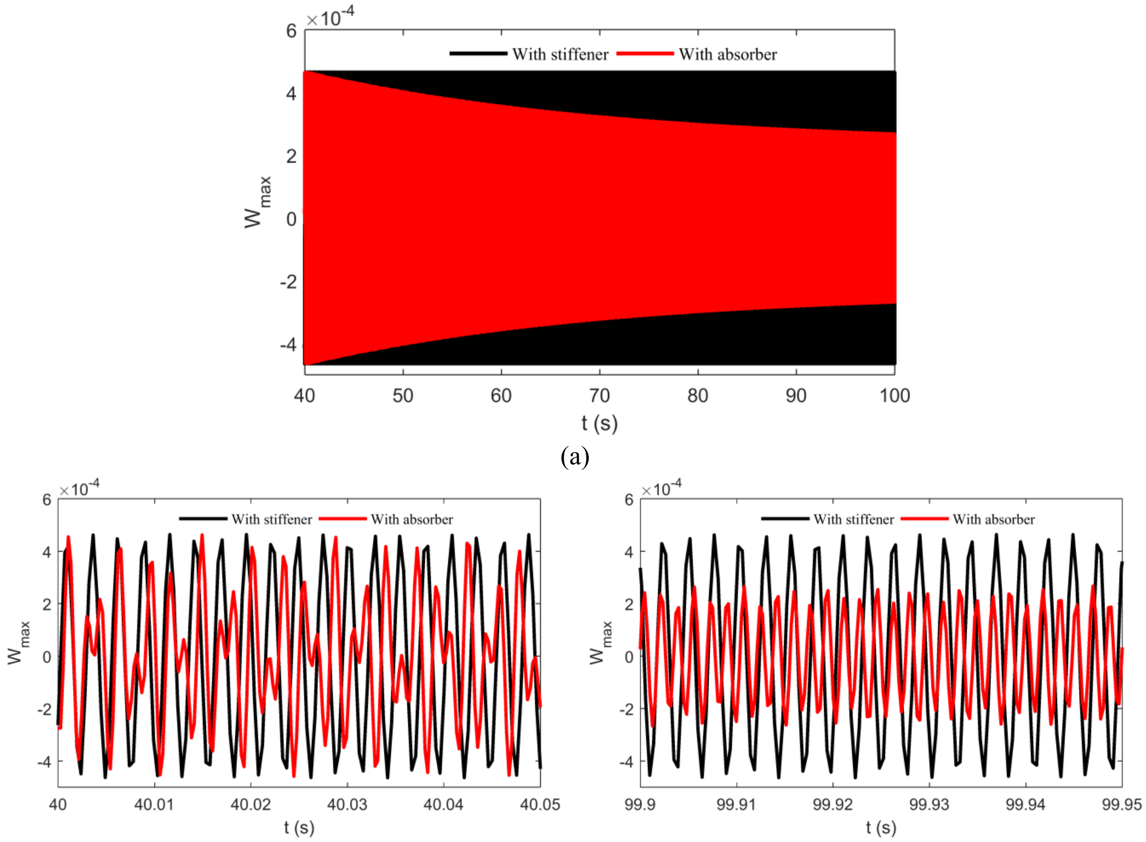

(a)

(b) The first periods

(c)The far periods

Fig. 4 Comparison of the effect of absorber without damper and siffener on the vibration response of FG cylindrical shell

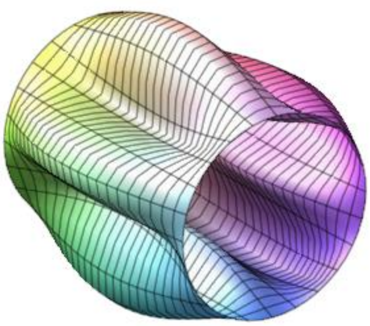

Fig. 5 The mode shapes of the FG cylindrical shell

For validating the present approach, in Table 1, the natural frequencies of simply supported cylindrical shell presented in this work are considered in comparison with the Pellicano (2007), Qin *et al.* (2017), and Wang *et al.* (2019c) results. Figs. 2 and 3 illustrate the results of the stiffened

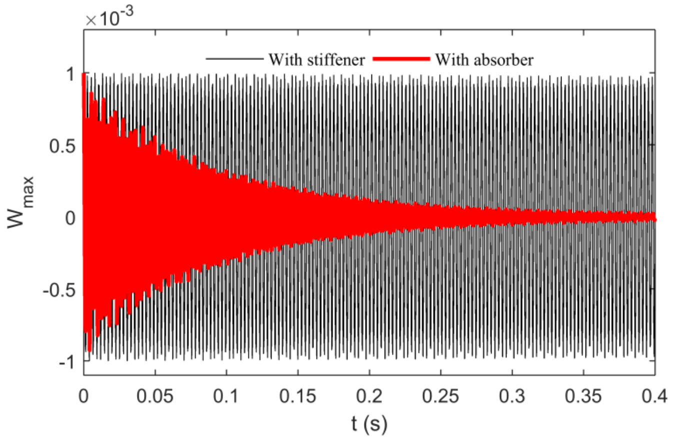

Fig. 6 The effect of absorber with local damper on the vibration response of FG cylindrical shell

and unstiffened cylindrical shell which are compared with the experimentally results of Sewall and Naumann (1968) and Sewall *et al.* (1964). Comparisons show that good conformance is obtained.

3.1 Vibration responses of SFG cylindrical shell

Here, the effect of vibration absorber on the vibration response of SFG cylindrical shells is illustrated. The influence of internal stiffeners, volume fraction, various locations of vibration absorbers, damping coefficient, and the periodic load on the vibration behaviors of SFG system are demonstrated. In this study, the number of stiffeners is considered to be thirty. The SFG cylindrical shell is considered to be made of alumina (Al_2O_3) and aluminum (Al) with the following material properties

$$Al: \ E_m = 70\,\mathrm{GPa}, \quad \rho_m = 2702\frac{\mathrm{Kg}}{\mathrm{m}^3}, \quad \nu_m = 0.3$$

$$Al_2O_3: \ E_c = 380\,\mathrm{GPa}, \quad \rho_c = 3800\frac{\mathrm{Kg}}{\mathrm{m}^3}, \quad \nu_c = 0.3$$

The Poisson's ratio for ceramic and metal is considered to be equal (i.e., $\nu=\nu_m=\nu_c=0.3$). The geometrical characteristics of the stiffeners and shell with FG material are as follows

$$\text{Shell:} \quad h = 0.002 \ \text{m}, \quad L = 0.75 \ \text{m}, \quad R = 0.5 \ \text{m}$$

$$\text{Stiffener:} \quad h_s = 0.01 \ \text{m}, \quad d_s = 0.0025 \ \text{m}$$

The parameters of the dynamic vibration absorber at $d = L/2$ can be written as follows

$$k = 5.3 \times 10^6 \ \frac{\mathrm{N}}{\mathrm{m}}, \quad c = 30 \ \frac{\mathrm{Ns}}{\mathrm{m}}, \quad M = 0.5 \ \text{kg}$$

The initial condition for shell deflection and vibration absorber variable are assumed to be equal to 0.001. In all solved examples, the number of full in the circumferential direction and half wave in the axial direction (n, m), which are not addressed in the simulation results, are considered to be equal to 5 and 1, respectively. It should be noted that the critical mode number is $n = 5$.

The effect of vibration absorber without damper and the stiffeners on the vibration behavior of

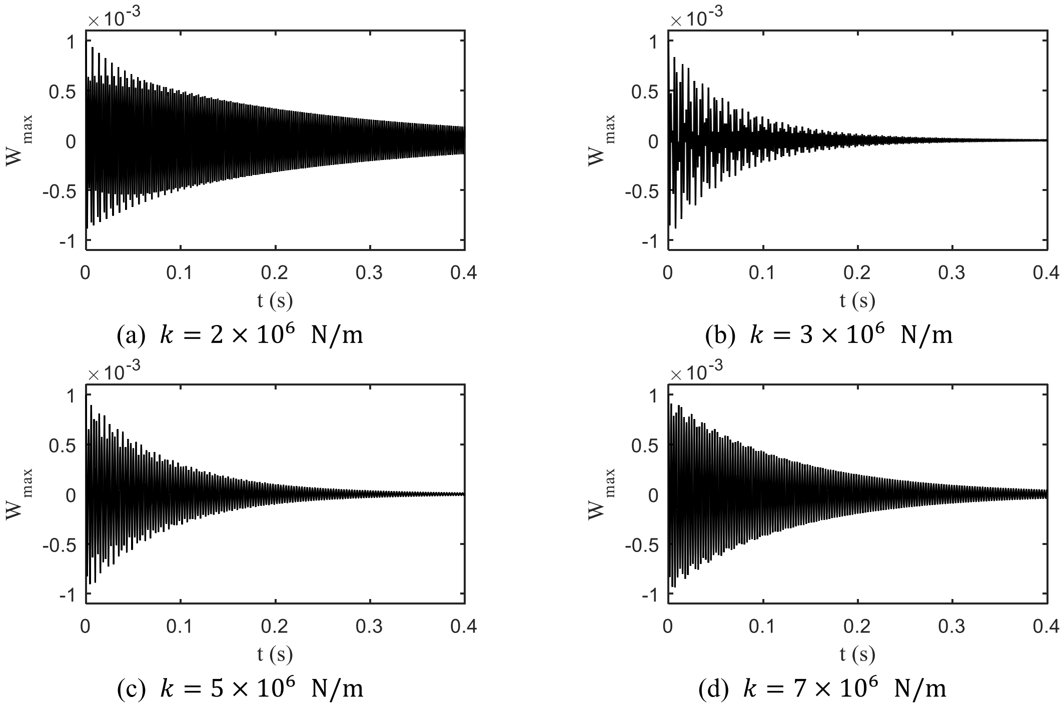

(a) $k = 2 \times 10^6$ N/m (b) $k = 3 \times 10^6$ N/m

(c) $k = 5 \times 10^6$ N/m (d) $k = 7 \times 10^6$ N/m

Fig. 7 The effect of different spring stiffness on the vibration responses of FG cylindrical shell

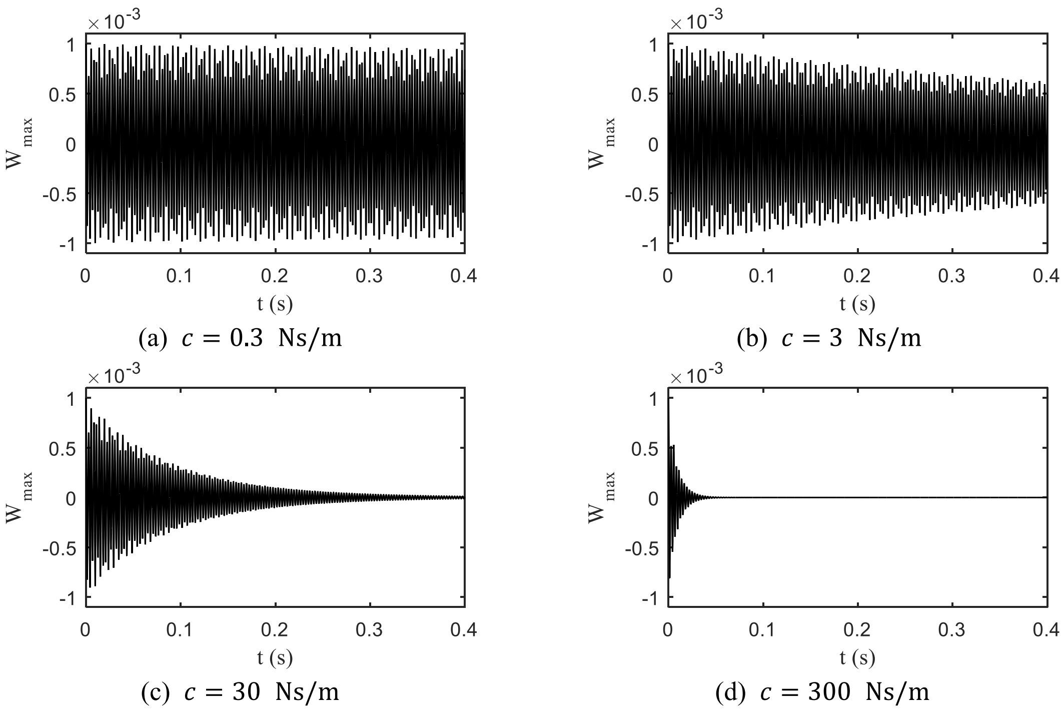

(a) $c = 0.3$ Ns/m (b) $c = 3$ Ns/m

(c) $c = 30$ Ns/m (d) $c = 300$ Ns/m

Fig. 8 The effect of various damping coefficients on the vibration responses of FG cylindrical shell

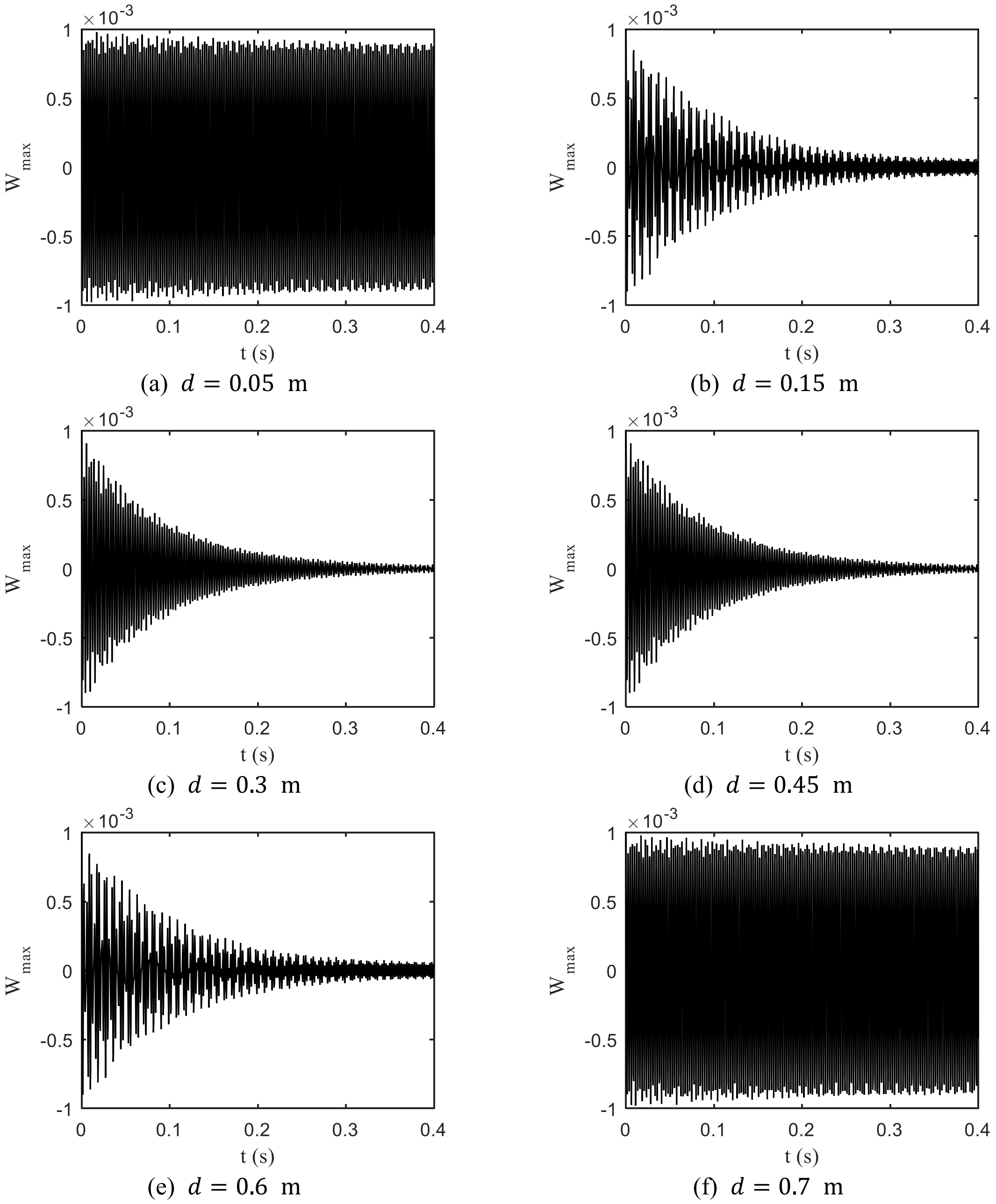

(a) $d = 0.05$ m (b) $d = 0.15$ m

(c) $d = 0.3$ m (d) $d = 0.45$ m

(e) $d = 0.6$ m (f) $d = 0.7$ m

Fig. 9 The effect of vibration absorbers on the different places of FG cylindrical shell

the FG cylindrical shell are illustrated in Fig. 4(a). Also, the vibration response in the first and far periods is shown in Figs. 4(b) and 4(c), respectively. According to Fig. 4, the vibration absorber is better performance than the stiffeners on decreasing the maximum deflection of system. In Fig. 5, the mode shapes of cylindrical shell with FG material are also illustrated.

The effect of vibration absorber with a local damper on the vibration response of the SFG

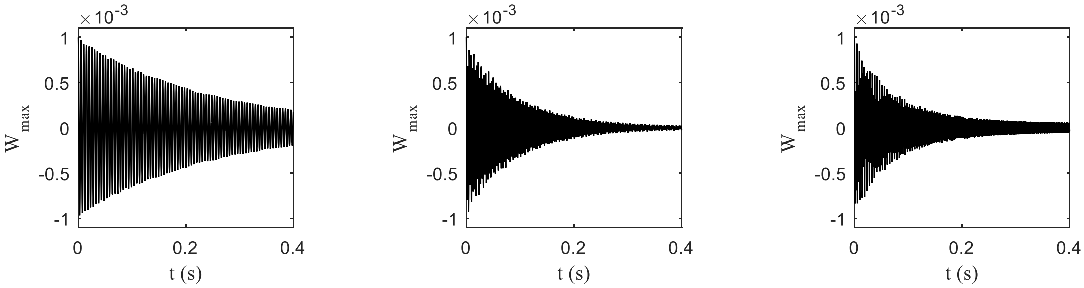

(a) Metal (b) FGM (c) Ceramic

Fig. 10 The effect of material composition of FG cylindrical shell on the vibration responses

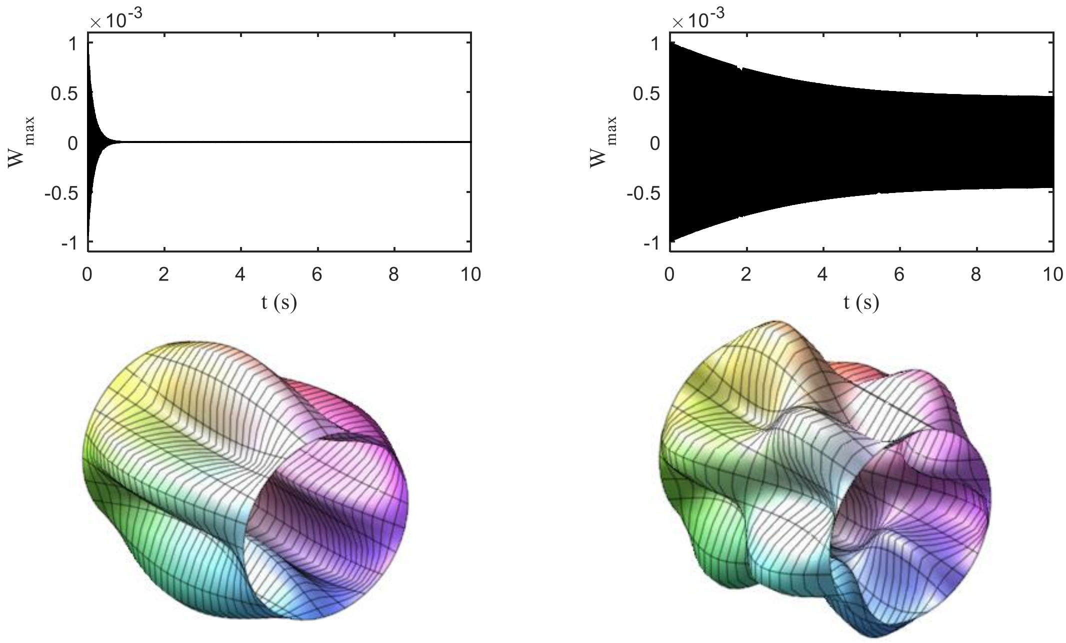

(a) $m = 1$ (b) $m = 2$

Fig. 11 The effect of different half waves (m) on the vibration responses ($n = 5$)

cylindrical shell is illustrated in Fig. 6. It is observed that the effect of the vibration absorber with a local damper on decreasing the maximum deflection of stiffened FG cylindrical shell is much higher than the absorber without damper.

The effect of the different spring stiffness on the vibration of the SFG cylindrical shell is illustrated in Fig. 7. According to this figure, the effect of spring stiffness increases the maximum deflection of stiffened FG cylindrical shell when the spring stiffness is far $k = 5 \times 10^6$ N/m. So, the spring stiffness about $k = 5 \times 10^6$ N/m is the best case and it can be decreased the maximum deflection of the system.

In Fig. 8 the vibration response with the various damping coefficients is shown. According to this figure, the maximum deflection of the SFG cylindrical shell decreases when the linear damping coefficient increases.

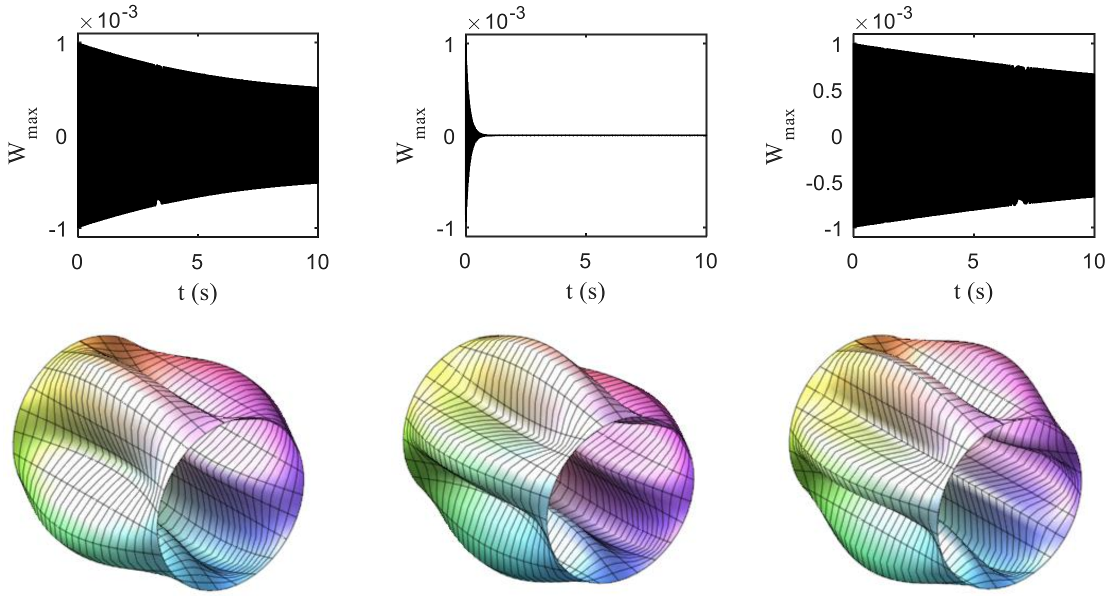

(a) $n = 4$ (b) $n = 5$ (c) $n = 6$

Fig. 12 The effect of different full wave (n) on the vibration responses ($m = 1$)

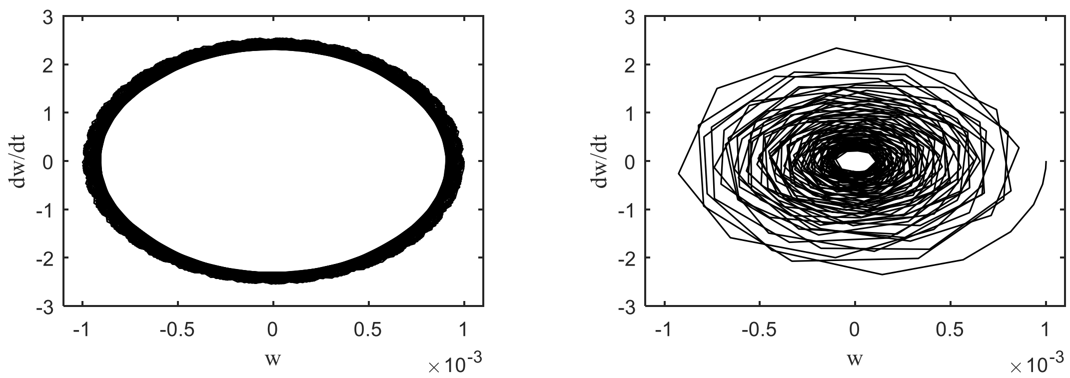

(a) Without vibration absorber (b) With vibration absorber

Fig. 13 Maximum deflection-velocity relation of FG cylindrical shell

In Fig. 9, the influence of vibration absorbers on the different positions of the SFG system is considered. According to this figure, the best position of vibration absorber is close to the center of the shell. So, the maximum deflection can be significantly decreased by considering a vibration absorber in the middle of the shell.

According to Fig. 10, the effect of vibration absorber on decreasing the maximum deflection for the metal shell is higher than the ceramic shell. According to these figures, metallic shell and FG shell have the highest and the lowest maximum deflection of the vibration response, respectively. Also, the maximum deflection of the FG shell is smaller than the ceramic and metallic shell.

In Figs. 11 and 12 the effect of half and full waves on the vibration response of the SFG system is considered. Regarding these figures, when $m = 1$ and $n = 5$, the maximum deflection can be significantly decreased. Also, the mode shapes of the FG cylindrical shell is shown in these figures.

The phase plane of forced vibration without and with vibration absorber is illustrated in Fig. 13, respectively. According to this figure, for the stiffened FG cylindrical shell without the vibration absorber, the relation of maximum deflection versus velocity has a closed curve while by considering the vibration absorber on the stiffened FG cylindrical shell, at first, the curve of maximum deflection versus velocity has disorder but when the time passes, it approaches to a limited cycle. Comparison of Fig. 13(a) and 13(b) illustrates that maximum deflection of stiffened FG cylindrical shell with vibration absorber has significantly decreased. For example, due to Figs. 13(a) and 13(b), the maximum deflection of stiffened FG cylindrical shell in steady state situation is decreased from 0.001 m to 0.0002 m.

4. Conclusions

A numerical method was utilized to study the influence of the new vibration absorber on the vibration behavior of SFG cylindrical shells under a couple of axial and transverse compression. The material composition stiffeners and shell is continuously changed through the thickness. The dynamic mass-spring-damper absorber is connected to the ground utilizing a linear local damper. The spring element of the vibration absorber is called global potential, which is connected to the FG cylindrical shell. The relations of strain-displacement are used according to the von Kármán equations and the classical shell theory. To consider the stiffeners in the model, the technique of smeared stiffener is utilized. After obtaining the governing equations, the Galerkin method is utilized to discretize the nonlinear dynamic equation of system. Also, In order to find the nonlinear vibration responses, the fourth order Runge-Kutta method is utilized. The influence of material properties, geometrical characteristics on the vibration response of system was investigated. Some of the main conclusions may be summarized as

• The vibration absorber is better performance than the stiffeners on decreasing the maximum deflection of cylindrical shell with FG material.

• The effect of the vibration absorber with a local damper on decreasing the maximum deflection of stiffened FG cylindrical shell is much higher than the absorber without damper.

• The spring stiffness about $k = 5 \times 10^6\ \mathrm{N/m}$, is the best case and it can be decreased the maximum deflection of SFG cylindrical shell.

• The maximum deflection of the FG shell is smaller than the ceramic and metallic shell.

• The maximum deflection of the SFG cylindrical shell decreases when the linear damping coefficient (c) increases.

• The maximum deflection can be significantly decreased by considering a vibration absorber in the middle of the shell.

References

Bich, D.H., Nam, V.H. and Phuong, N.T. (2011), “Nonlinear postbuckling of eccentrically stiffened functionally graded plates and shallow shells”, *Vietnam J. Mech.*, **33**(3), 131-147. https://doi.org/10.15625/0866-7136/33/3/207.

Bich, D.H., Van Dung, D. and Nam, V.H. (2012), "Nonlinear dynamical analysis of eccentrically stiffened functionally graded cylindrical panels", *Compos. Struct.*, **94**(8), 2465-2473. https://doi.org/10.1016/j.compstruct.2012.03.012.

Bich, D.H., Van Dung, D., Nam, V.H. and Phuong, N.T. (2013), "Nonlinear static and dynamic buckling analysis of imperfect eccentrically stiffened functionally graded circular cylindrical thin shells under axial compression", *Int. J. Mech. Sci.*, **74**, 190-200. https://doi.org/10.1016/j.ijmecsci.2013.06.002.

Duc, N.D. and Thang, P.T. (2015), "Nonlinear dynamic response and vibration of shear deformable imperfect eccentrically stiffened S-FGM circular cylindrical shells surrounded on elastic foundations", *Aerosp. Sci. Technol.*, **40**, 115-127. https://doi.org/10.1016/j.ast.2014.11.005.

Ebrahimi, F. and Heidari, E. (2018), "Surface effects on nonlinear vibration and buckling analysis of embedded FG nanoplates via refined HOSDPT in hygrothermal environment considering physical neutral surface position", *Adv. Aircraft Spacecraft Sci.*, **5**(6), 691-729. https://doi.org/10.12989/aas.2018.5.6.691.

Foroutan, K., Shaterzadeh, A. and Ahmadi, H. (2018), "Nonlinear dynamic analysis of spiral stiffened functionally graded cylindrical shells with damping and nonlinear elastic foundation under axial compression", *Struct. Eng. Mech.*, **66**(3), 295-303. https://doi.org/10.12989/sem.2018.66.3.295.

Foroutan, K., Shaterzadeh, A. and Ahmadi, H. (2019), "Nonlinear dynamic analysis of spiral stiffened cylindrical shells rested on elastic foundation", *Steel Compos. Struct.*, **32**(4), 509-519. https://doi.org/10.12989/scs.2019.32.4.509.

Foroutan, K., Shaterzadeh, A. and Ahmadi, H. (2020), "Nonlinear static and dynamic hygrothermal buckling analysis of imperfect functionally graded porous cylindrical shells", *Appl. Math. Model.*, **77**, 539-553. https://doi.org/10.1016/j.apm.2019.07.062.

Gonçalves, P.B. and Del Prado, Z.J. (2005), "Low-dimensional Galerkin models for nonlinear vibration and instability analysis of cylindrical shells", *Nonlinear Dynam.*, **41**(1-3), 129-145. https://doi.org/10.1007/s11071-005-2802-3.

Hong, C. (2014), "Rapid heating induced vibration of circular cylindrical shells with magnetostrictive functionally graded material", *Arch. Civ. Mech. Eng.*, **14**(4), 710-720. http://doi.org/10.1016/j.acme.2013.10.012.

Huang, H. and Han, Q. (2010), "Nonlinear dynamic buckling of functionally graded cylindrical shells subjected to time-dependent axial load", *Compos. Struct.*, **92**(2), 593-598 https://doi.org/10.1016/j.compstruct.2009.09.011.

Huang, Y. and Fuller, C. (1997), "The effects of dynamic absorbers on the forced vibration of a cylindrical shell and its coupled interior sound field", *J. Sound Vib.*, **200**(4), 401-418. https://doi.org/10.1006/jsvi.1996.0708.

Huang, Y.M. and Chen, C.C. (2000), "Optimal design of dynamic absorbers on vibration and noise control of the fuselage", *Comput. Struct.*, **76**(6), 691-702. https://doi.org/10.1016/S0045-7949(99)00190-X.

Meng, H., Han, Z.J. and Lu, G.Y. (2016), "Non-axisymmetric dynamic buckling of Cylindrical Shells under Axial Step Load", *Adv. Mater. Sci. Eng.*, 157-163. https://doi.org/10.1142/9789813141612_0021.

Ng, T., Lam, K., Liew, K. and Reddy, J. (2001), "Dynamic stability analysis of functionally graded cylindrical shells under periodic axial loading", *Int. J. Solids Struct.*, **38**(8), 1295-1309. https://doi.org/10.1016/S0020-7683(00)00090-1.

Pandy, M.G. and Koss, L. (1984), "Admittance-matched structures for the reduction of noise in tank making operations", *J. Sound Vib.*, **95**(2), 261-279. https://doi.org/10.1016/0022-460X(84)90547-9.

Pellicano, F. (2007), "Vibrations of circular cylindrical shells: Theory and experiments", *J. Sound Vib.*, **303**(1-2), 154-170. https://doi.org/10.1016/j.jsv.2007.01.022.

Qin, Z., Chu, F. and Zu, J. (2017), "Free vibrations of cylindrical shells with arbitrary boundary conditions: A comparison study", *Int. J. Mech. Sci.*, **133**, 91-99. https://doi.org/10.1016/j.ijmecsci.2017.08.012.

Sayyad, A.S. and Ghugal, Y.M. (2018), "An inverse hyperbolic theory for FG beams resting on Winkler-Pasternak elastic foundation", *Adv. Aircraft Spacecraft Sci.*, **5**(6), 671-689. https://doi.org/10.12989/aas.2018.5.6.671.

Sewall, J.L. and Naumann, E.C. (1968), "An experimental and analytical vibration study of thin cylindrical shells with and without longitudinal stiffeners", NASA TN D-4705, National Aeronautics and Space

Administration.
Sewall, J.L., Clary, R.R. and Leadbetter, S.A. (1964), "An experimental and analytical vibration study of a ring-stiffened cylindrical shell structure with various support conditions", NASA TN D-2398, National Aeronautics and Space Administration.
Shaterzadeh, A., Foroutan, K. and Ahmadi, H. (2019), "Nonlinear static and dynamic thermal buckling analysis of spiral stiffened functionally graded cylindrical shells with elastic foundation", *Int. J. Appl. Mech.*, **11**(1), 1950005. https://doi.org/10.1142/S1758825119500054.
Shegokara, N.L. and Lal, A. (2016), "Stochastic dynamic instability response of piezoelectric functionally graded beams supported by elastic foundation", *Adv. Aircraft Spacecraft Sci.*, **3**(4), 471-502. https://doi.org/10.12989/aas.2016.4.3.471.
Sofiyev, A. and Schnack, E. (2004), "The stability of functionally graded cylindrical shells under linearly increasing dynamic torsional loading", *Eng. Struct.*, **26**(10), 1321-1331. https://doi.org/10.1016/j.engstruct.2004.03.016.
Sofiyev, A.H. (2004), "The stability of functionally graded truncated conical shells subjected to aperiodic impulsive loading", *Int. J. Solids Struct.*, **41**(13), 3411-3424. https://doi.org/10.1016/j.ijsolstr.2004.02.003.
Sofiyev, A.H. (2009), "The vibration and stability behavior of freely supported FGM conical shells subjected to external pressure", *Compos. Struct.*, **89**(3), 356-366. https://doi.org/10.1016/j.compstruct.2008.08.010.
Turco, E. and Gardonio, P. (2017), "Sweeping shunted electro-magnetic tuneable vibration absorber: Design and implementation", *J. Sound Vib.*, **407**, 82-105. https://doi.org/10.1016/j.jsv.2017.06.035.
Van Dung, D. and Nam, V.H. (2014), "Nonlinear dynamic analysis of eccentrically stiffened functionally graded circular cylindrical thin shells under external pressure and surrounded by an elastic medium", *Eur. J. Mech. A Solid.*, **46**, 42-53. https://doi.org/10.1016/j.euromechsol.2014.02.008.
Volmir, A.S. (1972), *Non-linear Dynamics of Plates and Shells*, AS Science Edition M, USSR.
Wang, Y., Ye, C. and Zu, J.W. (2018), "Identifying the temperature effect on the vibrations of functionally graded cylindrical shells with porosities", *Appl. Math. Mech.*, **39**(11), 1587-1604. https://doi.org/10.1007/s10483-018-2388-6.
Wang, Y.Q. (2014), "Nonlinear vibration of a rotating laminated composite circular cylindrical shell: traveling wave vibration", *Nonlinear Dynam.*, **77**(4), 1693-1707. https://doi.org/10.1007/s11071-014-1410-5.
Wang, Y.Q. (2018), "Electro-mechanical vibration analysis of functionally graded piezoelectric porous plates in the translation state", *Acta Astronaut.*, **143**, 263-271. https://doi.org/10.1016/j.actaastro.2017.12.004.
Wang, Y.Q. and Yang, Z. (2017), "Nonlinear vibrations of moving functionally graded plates containing porosities and contacting with liquid: internal resonance", *Nonlinear Dynam.*, **90**(2), 1461-1480. https://doi.org/10.1007/s11071-017-3739-z.
Wang, Y.Q. and Zu, J.W. (2017a), "Vibration behaviors of functionally graded rectangular plates with porosities and moving in thermal environment", *Aerosp. Sci. Technol.*, **69**, 550-562. https://doi.org/10.1016/j.ast.2017.07.023.
Wang, Y.Q. and Zu, J.W. (2017b), "Nonlinear steady-state responses of longitudinally traveling functionally graded material plates in contact with liquid", *Compos. Struct.*, **164**, 130-144. https://doi.org/10.1016/j.compstruct.2016.12.053.
Wang, Y.Q., Huang, X.B. and Li, J. (2016), "Hydroelastic dynamic analysis of axially moving plates in continuous hot-dip galvanizing process", *Int. J. Mech. Sci.*, **110**, 201-216. https://doi.org/10.1016/j.ijmecsci.2016.03.010.
Wang, Y.Q., Liang, L. and Guo, X.H. (2013), "Internal resonance of axially moving laminated circular cylindrical shells", *J. Sound Vib.*, **332**(24), 6434-6450. https://doi.org/10.1016/j.jsv.2013.07.007.
Wang, Y.Q., Wan, Y.H. and Zu, J.W. (2019a), "Nonlinear dynamic characteristics of functionally graded sandwich thin nanoshells conveying fluid incorporating surface stress influence", *Thin Wall. Struct.*, **135**, 537-547. https://doi.org/10.1016/j.tws.2018.11.023.
Wang, Y.Q., Ye, C. and Zu, J.W. (2019b), "Nonlinear vibration of metal foam cylindrical shells reinforced with graphene platelets", *Aerosp. Sci. Technol.*, **85**, 359-370. https://doi.org/10.1016/j.ast.2018.12.022.
Wang, Y.Q., Ye, C. and Zu, J.W. (2019c), "Vibration analysis of circular cylindrical shells made of metal

foams under various boundary conditions", *Int. J. Mech. Mater. Des.*, **15**(2), 333-344. https://doi.org/10.1007/s10999-018-9415-8.
Zenkour, A.M. and Aljadani, M.H. (2018), "Mechanical buckling of functionally graded plates using a refined higher-order shear and normal deformation plate theory", *Adv. Aircraft Spacecraft Sci.*, **5**(6), 615-632. https://doi.org/10.12989/aas.2018.5.6.615.

EC

Appendix

$$
\begin{aligned}
&A_{11}^{*}=\frac{1}{\Delta}A_{11},\ A_{22}^{*}=\frac{1}{\Delta}A_{22},\ A_{12}^{*}=\frac{A_{12}}{\Delta},\ A_{33}^{*}=\frac{1}{A_{33}},\ \Delta=A_{11}A_{22}-A_{12}^{2}\\
&A_{14}^{*}=A_{22}^{*}A_{14}-A_{12}^{*}A_{15},\ A_{25}^{*}=A_{11}^{*}A_{25}-A_{12}^{*}A_{15},\ A_{15}^{*}=A_{22}^{*}A_{15}-A_{12}^{*}A_{25}\\
&A_{24}^{*}=A_{11}^{*}A_{15}-A_{12}^{*}A_{14},\ A_{36}^{*}=\frac{A_{36}}{A_{33}},\ A_{44}^{*}=A_{44}-A_{14}A_{14}^{*}-A_{15}A_{24}^{*}\\
&A_{55}^{*}=A_{55}-A_{25}A_{25}^{*}-A_{15}A_{15}^{*},\ A_{45}^{*}=A_{45}-A_{14}A_{15}^{*}-A_{15}A_{25}^{*}\\
&A_{54}^{*}=A_{45}-A_{25}A_{24}^{*}-A_{15}A_{14}^{*},\ A_{66}^{*}=A_{66}-A_{36}A_{36}^{*}
\end{aligned}
\tag{A1}
$$

where

$$
\begin{aligned}
&A_{11}=\frac{E_1}{1-\nu^2}+\frac{E_{1s}d_s}{S_s},\ A_{12}=\frac{E_1\nu}{1-\nu^2},\ A_{14}=\frac{E_2}{1-\nu^2}+\frac{E_{2s}d_s}{S_s}\\
&A_{15}=\frac{E_2\nu}{1-\nu^2},\ A_{22}=\frac{E_1}{1-\nu^2}+\frac{E_{1r}d_r}{S_r},\ A_{25}=\frac{E_2}{1-\nu^2}+\frac{E_{2r}d_r}{S_r}\\
&A_{33}=\frac{E_1}{2(1+\nu)},\ A_{36}=\frac{E_2}{2(1+\nu)},\ A_{44}=\frac{E_3}{1-\nu^2}+\frac{E_{3s}d_s}{S_s}\\
&A_{45}=\frac{E_3\nu}{1-\nu^2},\ A_{55}=\frac{E_3}{1-\nu^2}+\frac{E_{3r}d_r}{S_r},\ A_{66}=\frac{E_3}{2(1+\nu)}
\end{aligned}
\tag{A2}
$$

where

$$
\begin{aligned}
&E_1=\int_{-h/2}^{h/2}E_{sh}(z)dz=\left(E_m+\frac{E_c-E_m}{k+1}\right)h\\
&E_2=\int_{-h/2}^{h/2}zE_{sh}(z)dz=\frac{(E_c-E_m)kh^2}{2(k+1)(k+2)}\\
&E_3=\int_{-h/2}^{h/2}z^2E_{sh}(z)dz=\\
&\left[\frac{E_m}{12}+(E_c-E_m)\left(\frac{1}{k+3}-\frac{1}{k+2}+\frac{1}{4k+4}\right)\right]h^3\\
&E_{1i}=\int_{-h/2}^{h/2+h_i}E_i(z)dz=\left(E_c+\frac{E_m-E_c}{k_2+1}\right)h_i\\
&E_{2i}=\int_{-h/2}^{h/2+h_i}zE_i(z)dz=\frac{E_c}{2}hh_i\left(\frac{h_i}{h}+1\right)\\
&+(E_m-E_c)hh_i\left(\frac{1}{k_2+2}\frac{h_i}{h}+\frac{1}{2k_2+2}\right)\qquad ;\ i=s,r\\
&E_{3i}=\int_{-h/2}^{h/2+h_i}z^2E_i(z)dz=\frac{E_c}{3}h_i^3\left(\frac{3}{4}\frac{h^2}{h_i^2}+\frac{3}{2}\frac{h_i}{h}+1\right)\\
&+(E_m-E_c)h_i^3\left(\frac{1}{k_2+3}+\frac{1}{k_2+2}\frac{h}{h_i}+\frac{1}{4(k_2+1)}\frac{h^2}{h_i^2}\right)
\end{aligned}
\tag{A3}
$$